

RESEARCH ARTICLE

The change of longitudinal relaxation rate in oxygen enhanced pulmonary MRI depends on age and BMI but not diffusing capacity of carbon monoxide in healthy never-smokers

Simon Sven Ivan Kindvall^{1*}, Sandra Diaz², Jonas Svensson³, Per Wollmer⁴, Lars E. Olsson¹

1 Medical Radiation Physics, Translational Medicine, Lund University, Malmö, Sweden, **2** Medical Radiology, Translational Medicine, Lund University, Malmö, Sweden, **3** Medical Imaging and Physiology, Skane University Hospital, Lund, Sweden, **4** Clinical Physiology, Translational Medicine, Lund University, Malmö, Sweden

* Simon.kindvall@med.lu.se



OPEN ACCESS

Citation: Kindvall SSI, Diaz S, Svensson J, Wollmer P, Olsson LE (2017) The change of longitudinal relaxation rate in oxygen enhanced pulmonary MRI depends on age and BMI but not diffusing capacity of carbon monoxide in healthy never-smokers. PLoS ONE 12(5): e0177670. <https://doi.org/10.1371/journal.pone.0177670>

Editor: Peter Lundberg, Linköping University, SWEDEN

Received: August 31, 2016

Accepted: May 1, 2017

Published: May 11, 2017

Copyright: © 2017 Kindvall et al. This is an open access article distributed under the terms of the [Creative Commons Attribution License](https://creativecommons.org/licenses/by/4.0/), which permits unrestricted use, distribution, and reproduction in any medium, provided the original author and source are credited.

Data Availability Statement: The authors confirm that all data underlying the findings are fully available without restriction. All relevant data are within the Supporting Information files.

Funding: This work was supported by Allmänna Sjukhusets i Malmö stiftelse för bekämpande av cancer and Stiftelsen för cancerforskning vid onkologiska kliniken vid Universitetssjukhuset MAS. The funders had no role in study design, data

Abstract

Objective

Oxygen enhanced pulmonary MRI is a promising modality for functional lung studies and has been applied to a wide range of pulmonary conditions. The purpose of this study was to characterize the oxygen enhancement effect in the lungs of healthy, never-smokers, in light of a previously established relationship between oxygen enhancement and diffusing capacity of carbon monoxide in the lung ($D_{L,CO}$) in patients with lung disease.

Methods

In 30 healthy never-smoking volunteers, an inversion recovery with gradient echo read-out (Snapshot-FLASH) was used to quantify the difference in longitudinal relaxation rate, while breathing air and 100% oxygen, $\Delta R1$, at 1.5 Tesla. Measurements were performed under multiple tidal inspiration breath-holds.

Results

In single parameter linear models, $\Delta R1$ exhibit a significant correlation with age ($p = 0.003$) and BMI ($p = 0.0004$), but not $D_{L,CO}$ ($p = 0.33$). Stepwise linear regression of $\Delta R1$ yields an optimized model including an age-BMI interaction term.

Conclusion

In this healthy, never-smoking cohort, age and BMI are both predictors of the change in MRI longitudinal relaxation rate when breathing oxygen. However, $D_{L,CO}$ does not show a significant correlation with the oxygen enhancement. This is possibly because oxygen transfer in the lung is not diffusion limited at rest in healthy individuals. This work stresses the importance of using a physiological model to understand results from oxygen enhanced MRI.

collection and analysis, decision to publish, or preparation of the manuscript.

Competing interests: The authors have declared that no competing interests exist.

Introduction

In 2012, chronic obstructive pulmonary disease (COPD) alone was the third largest cause of death world-wide (3.1 million) [1] and the prevalence of COPD is predicted to increase over the next decades due to an ageing population and continued exposure of populations to risk factors such as tobacco smoke and pollutants [2]. Although COPD is a mix of chronic bronchitis and emphysema, which effects ventilation, perfusion and diffusion in a spatially heterogeneous manner, the disease is often classified according to spirometric pulmonary function tests (PFT) based on ventilation [2], with little regard to perfusion and diffusion of gases. In this context, oxygen enhanced (OE) -MRI is a promising modality for imaging pulmonary function [3]. As described in detail by Ohno and Hatabu [4], molecular oxygen will have the effect of a paramagnetic contrast agent in pulmonary blood according to $R_1 = R_{1,0} + r_{1,O_2} \cdot PO_2$, where $R_1 = 1/T_1$ is the measured longitudinal relaxation rate; $R_{1,0}$ is the baseline relaxation rate; PO_2 is the partial pressure, and r_{1,O_2} is the relaxivity, of oxygen. The relaxation enhancement (OE-effect), quantified as the change in relaxation rate between breathing air and oxygen, ΔR_1 , is claimed to be proportional to the corresponding change in oxygen partial pressure, ΔPO_2 [5]. The clinical relevance of OE-MRI has been previously attributed to a high correlation between OE (as signal enhancement) and the relative predicted carbon monoxide diffusing capacity of the lung (RP $D_{L,CO}$) [6,7].

During recent years, OE-MRI has successfully been used to study patients with COPD [8,9]; chronic lung allograft dysfunction [10]; interstitial lung disease [11]; and asthma [12] as well as a murine emphysema model [13]. Several centers have also used ultra-short echo time for OE-measurements, to address the inherently low MR-signal [14–16]. However, although OE-MRI has been applied to study disease and healthy controls [15,17], no previous work has described the effect with respect to age and sex in a healthy cohort. Moreover, the original description OE-effect as a pure relaxation enhancement [4], fails to take into account some physiological considerations:

A description of the OE effect often includes a previously reported (in 2002) dependency of OE on RP $D_{L,CO}$ in two mixed cohorts of patients and volunteers [6,7]. However, the transfer of oxygen in the healthy lung is perfusion limited at rest—in contrast to the transfer of carbon monoxide which is diffusion limited [18]—and the arterial PO_2 (Pa_{O_2}) has recently (in 2015) been shown to *not* be related to RP $D_{L,CO}$ in healthy individuals at rest [19]. It is important to note that Pa_{O_2} is expected to be the same as the pulmonary PO_2 , apart from the effects of physiological shunt.

As outlined in the Theory section, the OE effect is expected to depend on the volumes of pulmonary arterial and venous blood. Since the measured baseline lung T_1 has been shown to also depend on lung blood T_1 [20]; lung blood volume changes with age and sex [21]; and lung T_1 depends on age and sex [22]; the OE-effect in the lung will likely depend on age and sex.

Finally, Pa_{O_2} is known to vary with body mass index (BMI) even in non-obese subjects [23], with high-BMI subjects having a lower Pa_{O_2} [24]. This potentially makes BMI a predictor of the OE-effect in a healthy cohort, assuming that OE-measurements do indeed reflect the transfer of oxygen to the blood.

The purpose of this paper is to present and describe novel data on oxygen enhanced MRI, quantified by ΔR_1 , in the lungs of healthy never-smokers with respect to age, sex and BMI, and to evaluate the data in view of a previously reported relationship between the OE-effect and RP $D_{L,CO}$ [6,7].

Theory

The original description of OE-MRI relies on the paramagnetic effect of dissolved oxygen in blood, which would give a signal enhancement proportional to the change in oxygen partial pressure in lung blood [4]. However, this does not take into account the macromolecule dependent relaxivity of oxygen; the presence of deoxygenated (precapillary) blood in the lung; and the changes in blood volume that may come with oxygen breathing.

The relaxivity of molecular oxygen, r_{1,O_2} , is often cited to be $2.49 \times 10^{-4} \text{ s}^{-1} \text{ mmHg}^{-1}$ [8,25]; but this applies to distilled water [5], and the value in whole blood at 1.5 Tesla is likely between 3.38 to $4.38 \times 10^{-4} \text{ s}^{-1} \text{ mmHg}^{-1}$, depending on the erythrocyte volume fraction (EVF) [5,26,27]. The difference in O_2 -relaxivity between blood and water can be appreciated with the Bloomberg-Purcell-Pound relaxation theory, since para- and diamagnetic relaxation is synergistic [28,29]. Using a relaxivity value from whole blood, 0.41 EVF, $r_{1,O_2} = 4.1 \times 10^{-4} \text{ s}^{-1} \text{ mmHg}^{-1}$ [27], the ΔR_1 in pulmonary veins is expected to be approximately 0.2 s^{-1} for a 500 mmHg change in PO_2 —twice as much as reported in the lung [15]. However, while the ΔPO_2 in pulmonary veins is theoretically more than 500 mmHg, the ΔPO_2 in pulmonary arteries is close to 15 mmHg [18]. The blood relaxation in turn is quite well understood and described by a plasma- and erythrocyte-water compartment in fast exchange [30,31]. Thus, the pulmonary arterial compartment (deoxygenated blood) will exhibit a small *decrease* in R_1 with 100% oxygen breathing due to the oxygenation of hemoglobin [30,31]. Moreover, the overall blood content of the lung seems to increase with oxygen supplementation [32], and since the lung T1 is an echo time dependent mix of the lung parenchyma T1 and blood T1 [20], this mechanism will *decrease* the overall lung R_1 , but increase signal intensity. The observed *increase* in lung R_1 (global ΔR_1 on the order of 0.10 s^{-1}) is explained by the large signal contribution of oxygenated blood within most voxels of the lung.

Considering this, the OE-effect does depend on lung P_{O_2} ; but one must consider the total blood content and partitioning between the oxygenated/deoxygenated (pulmonary arterial/venous) blood compartments of the lung voxel where the T1-calculation is done.

Methods and materials

Subjects and hardware

With approval from the Regional Ethical Review Board, 31 never-smoking healthy subjects (16 male, 15 female) between 20–70 years were recruited to perform a clinical lung MRI examination, pulmonary function tests (PFT) and whole lung T₁ measurements with and without oxygen enhancement. Never-smokers were defined according to three criteria: a) never smoked daily for more than a month, b) smoking occasionally less than once a month, and c) reporting 0 pack-years of lifetime tobacco use. Subjects were provided with written instructions, signed informed consent, reported lifetime tobacco use, pulmonary health status and filled out a MRI safety sheet prior to the visit. The PFT was either made immediately after the MRI examination, or the next day. All MRI measurements were made on a 1.5 Tesla Siemens Magnetom AvantoFit (SIEMENS Healthcare, Erlangen, Germany), with an 18 channel body coil and a 32 channel spine matrix.

Clinical examination and PFT

All subjects underwent a morphological MRI examination, which included two full coverage coronal HASTE (Half-Fourier Acquisition Single shot Turbo Spin Echo) acquisitions during end-inspiration breath-hold and during free breathing respectively, as well as an axial VIBE acquisition during end-inspiration breath-hold. The images were examined by clinical

radiologists with 10 or 5 years of experience. Pulmonary function tests including measurements of total lung capacity (TLC), residual volume (RV), functional residual capacity (FRC), vital capacity (VC), forced expiratory volume in 1 second (FEV_1), $D_{L,CO}$, and $D_{L,CO}$ adjusted for alveolar volume (k_{CO}), were performed by clinical physiology personnel, using a Carefusion Masterscreen PFT and Body/Diffusion and the SentrySuite version 2.7 or higher (Carefusion Corporation, San Diego, CA). Relative predicted $D_{L,CO}$ was calculated using standard equations from the European community for steel and coal (ECSC) [33], other values are reported as nominal volumes.

T_1 -measurements and oxygen enhanced MRI

All T_1 measurements were made with the Snapshot FLASH pulse sequence [34] which is based on the Look and Locker sequence [35]. Following spin inversion, several gradient echo images are collected during magnetization recovery. Imaging parameters were as follows: matrix 128 x 64 zero filled to 256 x 256; 450 mm square field of view; 1.5 cm slice thickness; TE = 0.67 ms; TR = 3.0 ms; and flip angle = 7°. A non-selective hyperbolic secant pulse was used for spin inversion and Hanning-windowed sinc pulses with 1.6 sidelobes were used for image acquisition. One T_1 measurement is made in each slice; 16 gradient echo images with different inversion times are used in the calculation of the T_1 map; and the total measurement time is 3.0 seconds per slice. Each T_1 measurement was preceded by oral instructions for breath-hold after a tidal inspiration and subjects were given at least 10 seconds of free breathing in between measurements, which is also assumed to be enough to restore magnetization equilibrium for $T_1 < 2000$ ms.

T_1 mapping of the entire lung was performed at baseline and after 5 min inhalation of 100% oxygen. Medical air or oxygen was supplied at >10 l/min using a tight fitting oro-nasal mask with a non-rebreathing valve (V2-Mask 7450, T-Shape valve 2700, Hans Rudolph Co., Kansas City, MO), equipped with a 1 liter plastic reservoir bag and 40 cm low-resistance tubing (dead space in valve housing is 77 ml). Three sizes of masks were available to ensure optimal fit to each subject; each subject tried to inhale while shutting the air-inlet with their hand and reported no leakage prior to measurement.

To estimate the uncertainty of the measurements, a single slice is imaged repeatedly 10 times, using a rapid dynamic acquisition protocol with breath-hold [36].

Data processing

Data processing was made in MatLab R2014b (MathWorks, Natick, MA). The lungs were segmented in 3D using a region growing algorithm ("regionGrowing", Daniel Keller, 2011) or, in case the first algorithm fails, a slice by slice k-means clustering algorithm with five clusters. Either segmentation method was applied on a 3D image stack, containing the last magnitude image from the series of collected gradient echoes, followed by manual removal of major vessels. Segmentations were considered successful when each slice clearly included the signal magnitude gradient representing the border of the lung. The T_1 -value of the entire lung volume is defined as the center of a Gaussian curve, fitted to the histogram of all voxel values in the lung segmentation after a histogram thresholding [17,22]. Using the T_1 -values at baseline and after 5 min oxygen inhalation, the global difference in relaxation rate, ΔR_1 , was calculated for each subject.

Correcting for lung inflation

Using the segmented lung from the 3D-stack of magnitude images, the total lung volume at the time of measurement can be calculated. Since it is known that global T_1 varies with

lung inflation [17], the difference in lung volume between breathing oxygen and air, $\Delta V_L = V(\text{oxygen}) - V(\text{air})$, was calculated for each subject.

Statistical evaluation

Linear models of ΔR_1 , and ΔR_1 adjusted for age and sex, as a function of PFT-parameters were tested for 24 subjects with complete data. Linear models of general demographics: age, sex, height, weight and BMI, as well as ΔV_L were tested for the whole group of 30 subjects.

A stepwise linear regression is applied to a model of age, sex, BMI and ΔV_L —including first order interaction terms. Interaction terms are removed one by one based on the ANOVA p-value (likelihood that the estimate is separate from zero) to maximize the adjusted coefficient of determination (adj. R^2). The linear model ΔR_1 as a function of RP $D_{L,CO}$ is also tested for sex confounding and presented.

No correction is made for multiple testing and nominal p-values are used consequently.

Calculation of error bars

Using the rapid acquisition protocol [36] during steady state, 9 images of a single central slice are collected and the coefficient of variation (CV) of the mean R_1 in a circular ROI in the top right lung is calculated. The error bars represent $\pm CV \times R_1(\text{air})$ for each subject.

Results

All subjects completed the MRI examinations; six subjects were not able to complete the PFT due to logistical reasons; one subject was completely excluded due to clinical findings. General demographics and PFT measurements of the cohort has been presented earlier [22].

Plain unregistered maps of $\Delta R_1 = R_{1,\text{oxygen}} - R_{1,\text{air}}$ are presented in Fig 1 for representative females and males of age <30 and age >45. It is interesting to note that the pulmonary trunk and arteries exhibit negative enhancement ($R_{1,\text{oxygen}} < R_{1,\text{air}}$) in most subjects. The hypo/hyperintense regions close to the diaphragm result from misalignment between oxygen and air-images which is not corrected for at this stage, since difference images are not used in any calculations. The R^2 and p-values of single parameter linear models, and age- and sex-adjusted models, of nominal PFT parameters are presented in Table 1, for 24 subjects with complete PFT.

The mean ΔR_1 for 30 subjects is 0.11 s^{-1} with SD 0.021 s^{-1} . Single parameter linear models of age, sex, height, weight, BMI and ΔV_L are presented in Table 2, for all 30 subjects. The linear model ΔR_1 versus age yields a statistically significant slope of $-0.00076 \text{ s}^{-1} \text{ year}^{-1}$ (95% CI $[-0.0012 - 0.00029] \text{ s}^{-1} \text{ year}^{-1}$, $p = 0.003$, $n = 30$) corresponding to a 6.9% decrease in ΔR_1 in 10 years. The linear model ΔR_1 versus BMI yields a statistically significant slope of $-0.00431 \text{ s}^{-1} (\text{kg m}^{-2})^{-1}$ (95% CI $[-0.0065 - 0.0021] \text{ s}^{-1} (\text{kg m}^{-2})^{-1}$, $p = 0.0004$, $n = 30$) corresponding to 3.9% decrease in ΔR_1 for one BMI unit. Sex alone is not a significant predictor for ΔR_1 in the whole group (T-test, $p = 0.43$).

The final model contains sex, age, BMI, ΔV_L , and the BMI x age interaction term, where the removal of further terms will decrease the adjusted R^2 . The model is described by $\Delta R_1 = \Delta R_1(\text{male/female}) + C_1 \text{Age} + C_2 \text{BMI} + C_3 \text{Age} \times \text{BMI} + C_4 \Delta V_L$; has $R^2 = 0.66$ at $p = 5e-5$; and is presented in Fig 2, with model estimates in Table 3. It is important to note that ΔR_1 decreases with age and BMI, despite the C_{1-2} values being positive, and that the age-, BMI- and interaction-coefficients are not statistically different between sexes. It is also important to note that neither sex nor ΔV_L have an effect at $p < 0.05$, but including them raises the adjusted R^2 of the whole model. The mean CV of all subjects is 1.4%, $n = 30$. Since the CV for each subject is not

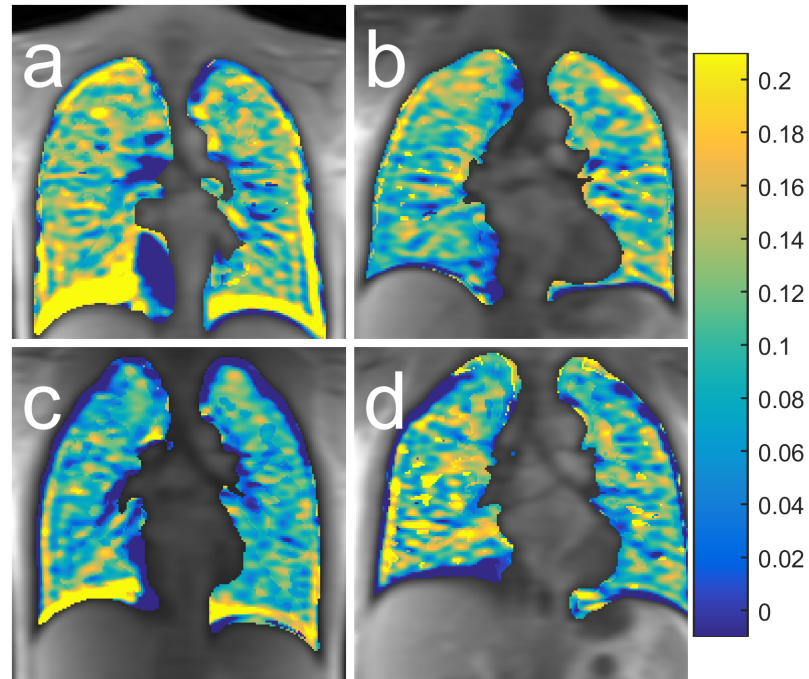


Fig 1. Oxygen enhancement images from four subjects. Representative maps of $\Delta R_1 = R_{1, \text{oxygen}} - R_{1, \text{air}}$ for a) Female age <30 years, b) Female age >45 years, c) Male age <30 years and d) Male age >45 years. The images are provided for completeness, and are not registered or processed.

<https://doi.org/10.1371/journal.pone.0177670.g001>

correlated with any of the variables age, BMI, sex, ΔV_L or ΔR_1 ($p > 0.3$), it is not incorporated in the statistical analysis, but only provided as a visual aid for interpretation.

A linear model of ΔR_1 as a function of RP $D_{L,CO}$ is not significant; $p = 0.33$, with slope $-0.00035 \text{ s}^{-1} [\%]^{-1}$ (95% CI $[-0.0011 \text{ } 0.00037] \text{ s}^{-1} [\%]^{-1}$). When allowing different baseline ΔR_1

Table 1. Values of R^2 for ΔR_1 as a function of pulmonary function test results for $n = 24$ subjects with complete pulmonary function tests. Unadjusted linear models, and models adjusted for age and sex are presented.

	Unadjusted:		Age and sex adj.:	
	R^2	P	R^2	P
Age+sex	0.35	0.011	---	---
Sex	0.032	0.407	---	---
Age	0.323	0.004	---	---
BMI	0.449	3.4e-3	0.599	3.2e-3
TLC	0.074	0.197	0.355	0.030
RV	0.291	0.007	0.365	0.026
FRC	0.005	0.742	0.392	0.017
VC	0.009	0.665	0.352	0.031
FEV ₁	0.023	0.477	0.351	0.031
$D_{L,CO}$	0.003	0.805	0.352	0.031
RP $D_{L,CO}$	0.043	0.333	0.349	0.032
K_{CO}	0.026	0.454	0.359	0.028

Abbreviations: body mass index, total lung capacity, residual volume, functional residual capacity, vital capacity, forced expiratory volume in 1 second, diffusing capacity of the lung for carbon monoxide ($D_{L,CO}$), relative predicted $D_{L,CO}$ and $D_{L,CO}$ corrected for alveolar volume

<https://doi.org/10.1371/journal.pone.0177670.t001>

Table 2. Values of R^2 for linear model of ΔR_1 versus general demographics, for $n = 30$ subjects.

	R^2	P-value
Sex	0.022	0.43
Age	0.28	0.0027
Height	0.008	0.63
Weight	0.28	0.0027
BMI	0.37	0.0004
ΔV_L	0.17	0.02

<https://doi.org/10.1371/journal.pone.0177670.t002>

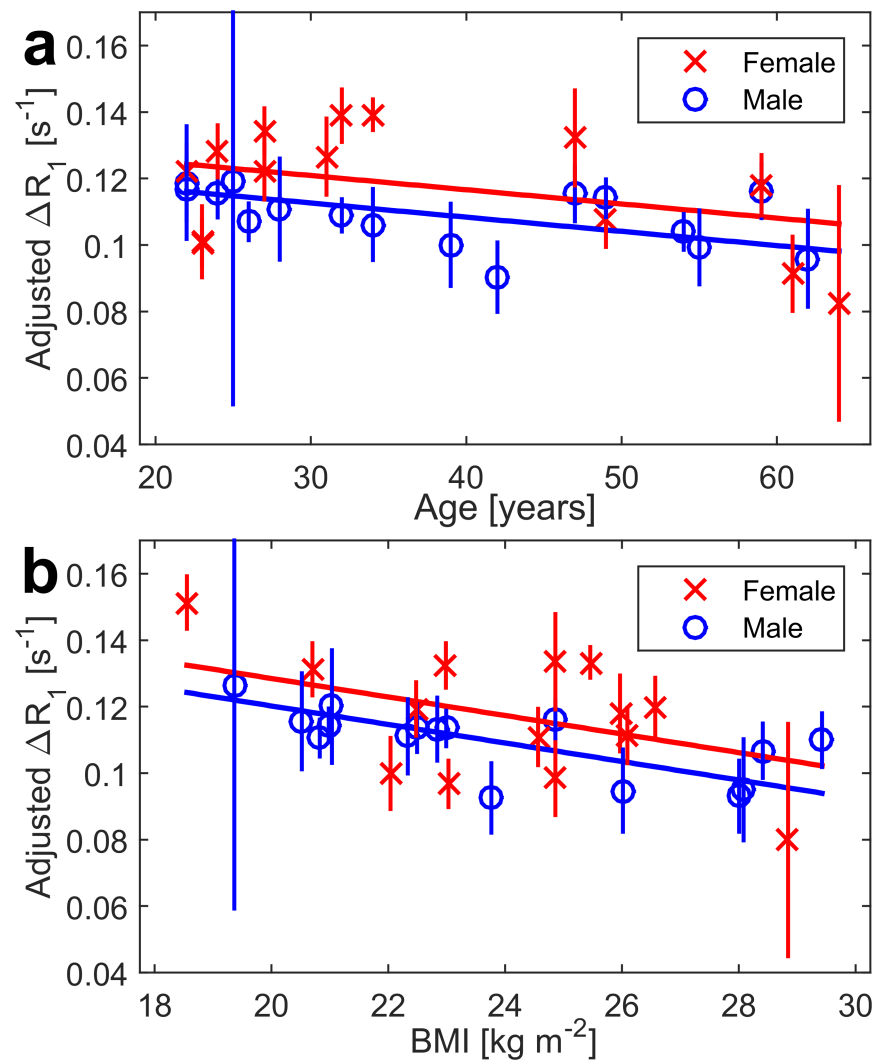


Fig 2. Main result plots of OE as a function of age and BMI. Equation: $\Delta R_1 = \Delta R_{1,0}(sex) + C_1 Age + C_2 BMI + C_3 Age \times BMI + C_4 \Delta V_L$, whole model R^2 is 0.66 at $p = 5e-5$ for $n = 30$ participants. Error bars represent the coefficient of variation in repeated measurements of R_1 a) ΔR_1 adjusted for BMI and ΔV_L as function of age and sex b) ΔR_1 adjusted for age and ΔV_L displayed as function of BMI.

<https://doi.org/10.1371/journal.pone.0177670.g002>

Table 3. Model parameters of $\Delta R_1 = \Delta R_1(\text{sex}) + C_1\text{Age} + C_2\text{BMI} + C_3\text{Age} \times \text{BMI} + C_4\Delta V_L$ for $n = 30$, with 95% confidence intervals.

	Estimate	95% CI	p-value
$\Delta R_{1,0}(\text{male}) [s^{-1}]$	0.0256	[-0.10 0.16]	0.69
$\Delta R_{1,0}(\text{female})[s^{-1}]$	0.0339	[-0.09 0.16]	0.59
$C_1 [s^{-1} y^{-1}] \times 10^{-3}$	3.97	[0.8 7.1]	0.017
$C_2 [s^{-1} kg^{-1} m^2] \times 10^{-3}$	4.20	[-1.3 9.7]	0.13
$C_3 [s^{-1} kg^{-1} m^2 y^{-1}] \times 10^{-3}$	-0.183	[-0.31–0.05]	0.008
$C_4 [s^{-1} l^{-1}] \times 10^{-3}$	10.8	[-7.3 29]	0.23

<https://doi.org/10.1371/journal.pone.0177670.t003>

based on sex, the effect of RP $D_{L,CO}$ on ΔR_1 is even smaller, with slope $-0.00027 s^{-1} [\%]^{-1}$ (95% CI $[-0.0011 0.00055] s^{-1} [\%]^{-1}$) at $p = 0.51$, and whole model $R^2 = 0.05$, Fig 3.

Discussion

In this study it has been shown that the oxygen enhancement as quantified by ΔR_1 decreases with age in a healthy population, with a more prominent decrease in subjects with high BMI. Moreover, ΔR_1 is not correlated to the relative predicted or nominal $D_{L,CO}$ (single breath, inert gas measurement), in our group of healthy never-smokers, which is congruent with current knowledge of oxygen diffusion in the lung [19].

The mean OE effect in the present study is similar to previous reported values of 0.08–0.12 s^{-1} [15], and the linear model used to describe the OE-effect seems feasible with respect to the physiological variations in the pulmonary circulation with age, BMI and sex [21,23].

Oxygen enhancement and $D_{L,CO}$

The lack of correlation between $D_{L,CO}$ and ΔR_1 in the healthy cohort is surprising at first; but in fact, Pa_{O_2} is not correlated to RP $D_{L,CO}$ at rest in healthy lungs [19], and a strong relationship

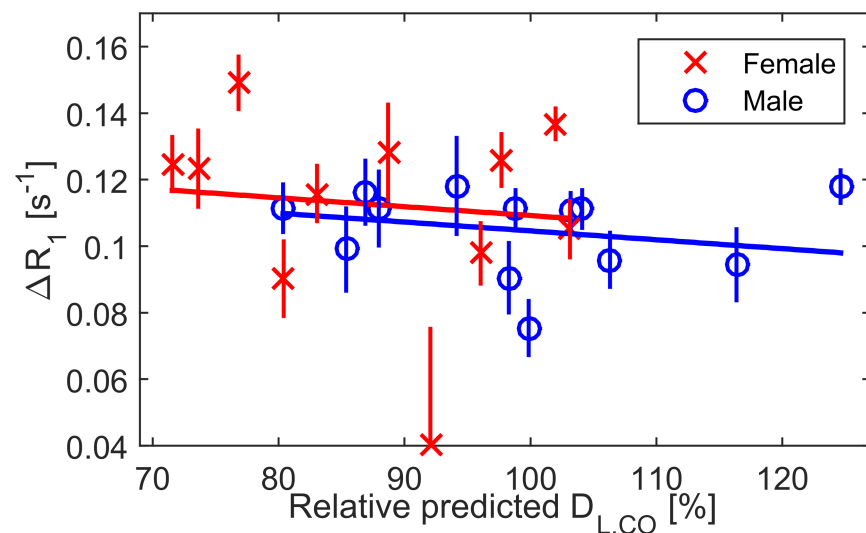


Fig 3. Plot of OE as a function of diffusing capacity. Linear regression of ΔR_1 as function of relative predicted $D_{L,CO}$ and sex for $n = 24$ participants, whole model R^2 is 0.05 at $p = 0.57$. Neither sex nor $D_{L,CO}$ is a significant predictor in this model. Error bars represent the coefficient of variation in repeated measurements of R_1 .

<https://doi.org/10.1371/journal.pone.0177670.g003>

between $D_{L,CO}$ and OE is only expected in very dysfunctional lungs or during exercise when oxygen transfer is diffusion limited [18]. A similar case is found in a recent article about T1 as a function of k_{CO} ($D_{L,CO}$ adjusted for alveolar volume) in healthy volunteers and COPD patients [37]; although the overall T1 vs. k_{CO} relationship is strong, the correlation is visibly close to zero for the healthy group alone [37]. Both cases are examples of Simpson's paradox [38], where a between-group regression is not necessarily valid within a group. It is possible that pathologic tissue change such as emphysema or fibrosis is a common cause for changes in T1, OE and $D_{L,CO}$ in diseased lungs, but that other physiological considerations are more important for the T1, OE and $D_{L,CO}$ in healthy lungs.

Oxygen enhancement and BMI and age

The arterial oxygen partial pressure will decrease with age and BMI [23], which logically will have a direct effect on the observed OE effect. A common hypothetical explanation for both the age and BMI dependency the OE effect is the closure of small airways, which produces micro-shunting [18]. The ageing lung loses elastic recoil (increased compliance) which aggravates this effect [18], and visceral fat may further compress the lung in the supine position and produce the age interaction. Shunting can in this context result in an increase in the deoxygenated fraction of lung blood of the given voxel, and in a decrease of the pulmonary venous blood P_{O_2} –creating a concurrent effect to lower the OE-effect.

The correlation between BMI and OE may also be a confounding effect of general physical fitness on both pulmonary function and BMI: a sedentary lifestyle or low physical activity increase BMI in overweight ($25 < \text{BMI} < 30$) individuals [39], and there is a positive dose-response relationship between physical activity and lung function as quantified by FEV_1 [40].

Limitations

A major limitation of the study is sample size, and the slightly skewed age distribution. However, since we required subjects to fill out a questionnaire about smoking, as outlined in the methods section, very few prospective volunteers born before the 70's identified themselves as never-smokers. The lung function as quantified by PFT is normal for all volunteers; residual volume increases with age ($\rho = 0.7$ at $p < 0.01$); and k_{CO} decreases with age ($\rho = -0.4$ at $p = 0.015$) [22]. The error bars represent the CV of the T1-measurement, which mostly depend on the subject's breathing technique. Respiratory phase can alter the T1-value by at least 6% [17], but the mean CV of the cohort presented here was lower than 2%, indicating that subsequent breath-holds resulted in a very similar lung volume. However, we did choose to correct for differences in lung inflation between oxygen and air measurements, which were separated by 5 minutes of free breathing to ensure gas equilibrium.

Previous work have only compared OE and the RP $D_{L,CO}$ [6,7], however, in the healthy cohort of the present study, none of the parameters RP $D_{L,CO}$, $D_{L,CO}$ or k_{CO} are significantly correlated with the measured OE-effect. As seen in Table 1, age and sex are much more potent predictors alone, and adding RP $D_{L,CO}$, $D_{L,CO}$ or k_{CO} has no impact on the model R^2 .

The OE measurement in this study was performed during a tidal inspiration breath-hold (FRC + tidal volume), and, as the magnitude of the OE effect likely depends on the respiratory phase [15], any work on the OE-effect during other parts of the respiratory cycle should take this into account. In this study, the difference in total volume of the segmented lung at air or oxygen measurement was used as a model parameter.

Finally, this entire paper has been regarding a *global* measure of the OE effect in the lungs of healthy individuals. When studying patients it is advisable to employ a method that allows the detection of regional heterogeneity, as this is expected in disease [8,10,13]. In this study,

coronal T1-maps were collected since this method allows the whole lung to be sampled in the shortest time. Ideally, OE-MRI should be performed with full lung coverage, as we have done, but with isotropic resolution to account for gravity dependent heterogeneity—which is expected even in the supine healthy lung [18].

Conclusion

Further studies should aim to improve the regional quantification possibilities of OE-MRI and describe the underlying physiological processes responsible for the changes in T1, OE and pulmonary function (such as $D_{L,CO}$) in the healthy and diseased lung. Eventually, a hemodynamic model of the lung is necessary to interpret all OE-MRI data—using either relaxation- or signal enhancement as end-points.

In conclusion, we have shown that OE-MRI as quantified by ΔR_1 varies with age and BMI, but not with relative predicted $D_{L,CO}$, in a healthy, never-smoking group. Moreover, a model including sex, age, BMI, lung volume and an age-BMI interaction is optimal, with respect to the adjusted R^2 -value, to describe the OE effect in this cohort. Thus, the influence of these variables should be considered in OE-studies of healthy volunteers or patients. The overall interpretation of the present study is that closure of small airways is more important for the OE-effect than gas diffusion, but more sophisticated experiments are needed to confirm this hypothesis.

Supporting information

S1 File. Supplementary raw data file. Anonymous data from all subjects are included for availability at the Journal's webpage.
(TXT)

Author Contributions

Conceptualization: LEO JS SD PW SK.

Data curation: SK.

Formal analysis: SK.

Funding acquisition: LEO SD.

Investigation: SK SD.

Methodology: SK LEO.

Project administration: LEO JS SD PW SK.

Resources: LEO SD.

Software: SK.

Supervision: LEO JS PW.

Validation: LEO JS SD PW SK.

Visualization: SK.

Writing – original draft: SK.

Writing – review & editing: LEO JS SD PW SK.

References

1. WHO. World Health Organization, The top 10 causes of death. In: Fact sheet N°310 [Internet]. World Health Organization; 2014 [cited 24 May 2016]. <http://www.who.int/mediacentre/factsheets/fs310/en/>
2. Vestbo J, Hurd SS, Agustí AG, Jones PW, Vogelmeier C, Anzueto A, et al. Global strategy for the diagnosis, management, and prevention of chronic obstructive pulmonary disease GOLD executive summary. *Am J Respir Crit Care Med*. 2013; 187: 347–365. <https://doi.org/10.1164/rccm.201204-0596PP> PMID: 22878278
3. Edelman RR, Hatabu H, Tadamura E, Li W, Prasad P V. Noninvasive Assessment of Regional ventilation in the human lung using oxygen-enhanced magnetic resonance imaging. *Nat Med*. 1996; 2: 1236–1239. PMID: 8898751
4. Ohno Y, Hatabu H. Basics concepts and clinical applications of oxygen-enhanced MR imaging. *Eur J Radiol*. 2007; 64: 320–8. <https://doi.org/10.1016/j.ejrad.2007.08.006> PMID: 17980535
5. Zaharchuk G, Busse RF, Rosenthal G, Manley GT, Glenn O a., Dillon WP. Noninvasive Oxygen Partial Pressure Measurement of Human Body Fluids In Vivo Using Magnetic Resonance Imaging. *Acad Radiol*. 2006; 13: 1016–1024. <https://doi.org/10.1016/j.acra.2006.04.016> PMID: 16843855
6. Ohno Y, Hatabu H, Takenaka D, Van Cauteren M, Fujii M, Sugimura K. Dynamic oxygen-enhanced MRI reflects diffusing capacity of the lung. *Magn Reson Med*. 2002; 47: 1139–44. <https://doi.org/10.1002/mrm.10168> PMID: 12111960
7. Müller CJ, Schwaiblmair M, Scheidler J, Deimling M, Weber J, Löffler RB, et al. Pulmonary diffusing capacity: assessment with oxygen-enhanced lung MR imaging preliminary findings. *Radiology*. 2002; 222: 499–506. <https://doi.org/10.1148/radiol.2222000869> PMID: 11818619
8. Morgan AR, Parker GJM, Roberts C, Buonaccorsi GA, Maguire NC, Hubbard Cristinacce PL, et al. Feasibility assessment of using oxygen-enhanced magnetic resonance imaging for evaluating the effect of pharmacological treatment in COPD. *Eur J Radiol*. 2014; 83: 2093–101. <https://doi.org/10.1016/j.ejrad.2014.08.004> PMID: 25176287
9. Jobst BJ, Triphan SMF, Sedlaczek O, Anjorin A, Kauczor HU, Biederer J, et al. Functional lung MRI in chronic obstructive pulmonary disease: comparison of t1 mapping, oxygen-enhanced t1 mapping and dynamic contrast enhanced perfusion. *PLoS One*. Public Library of Science; 2015; 10: e0121520.
10. Renne J, Lauermaun P, Hinrichs JB, Schönfeld C, Sorrentino S, Gutberlet M, et al. Chronic Lung Allograft Dysfunction: Oxygen-enhanced T1-Mapping MR Imaging of the Lung. *Radiology*. Radiological Society of North America Inc.; 2015; 276: 266–73.
11. Ohno Y, Nishio M, Koyama H, Yoshikawa T, Matsumoto S, Seki S, et al. Oxygen-enhanced MRI for patients with connective tissue diseases: comparison with thin-section CT of capability for pulmonary functional and disease severity assessment. *Eur J Radiol*. Elsevier Ireland Ltd; 2014; 83: 391–7.
12. Zhang W-J, Niven RM, Young SS, Liu Y-Z, Parker GJM, Naish JH. Dynamic oxygen-enhanced magnetic resonance imaging of the lung in asthma—Initial experience. *Eur J Radiol*. Elsevier Ireland Ltd; 2015; 84: 318–326.
13. Zurek M, Sladen L, Johansson E, Olsson M, Jackson S, Zhang H, et al. Assessing the Relationship between Lung Density and Function with Oxygen-Enhanced Magnetic Resonance Imaging in a Mouse Model of Emphysema. *PLoS One*. 2016; 11: e0151211. <https://doi.org/10.1371/journal.pone.0151211> PMID: 26977928
14. Zurek M, Johansson E, Risse F, Alamidi D, Olsson LE, Hockings PD. Accurate T(1) mapping for oxygen-enhanced MRI in the mouse lung using a segmented inversion-recovery ultrashort echo-time sequence. *Magn Reson Med*. John Wiley and Sons Inc.; 2014; 71: 2180–5.
15. Triphan SMF, Breuer FA, Gensler D, Kauczor H-U, Jakob PM. Oxygen enhanced lung MRI by simultaneous measurement of T1 and T2 * during free breathing using ultrashort TE. *J Magn Reson Imaging*. 2014; 41: 1708–14. <https://doi.org/10.1002/jmri.24692> PMID: 25044618
16. Kruger SJ, Fain SB, Johnson KM, Cadman R V, Nagle SK. Oxygen-enhanced 3D radial ultrashort echo time magnetic resonance imaging in the healthy human lung. *NMR Biomed*. 2014; 27: 1535–41. <https://doi.org/10.1002/nbm.3158> PMID: 24984695
17. Stadler A, Jakob PM, Griswold M, Barth M, Bankier A a. T1 mapping of the entire lung parenchyma: Influence of the respiratory phase in healthy individuals. *J Magn Reson Imaging*. 2005; 21: 759–64. <https://doi.org/10.1002/jmri.20319> PMID: 15906333
18. West JB. *Respiratory Physiology: The Essentials* [Internet]. 9:th Editi. Baltimore: Lippincott Williams & Wilkins; 2012. https://books.google.ca/books/about/Respiratory_Physiology.html?id=rHaZVmFZRvcC&pgis=1
19. Preisser AM, Seeber M, Harth V. Diffusion limitations of the lung—comparison of different measurement methods. *Adv Exp Med Biol*. 2015; 849: 65–73. https://doi.org/10.1007/5584_2014_90 PMID: 25381558

20. Triphan SMF, Jobst BJ, Breuer FA, Wielpütz MO, Kauczor H-U, Biederer J, et al. Echo time dependence of observed T 1 in the human lung. *J Magn Reson Imaging*. 2015; 42: 610–616. <https://doi.org/10.1002/jmri.24840> PMID: 25604043
21. Meinel FG, Graef A, Sommer WH, Thierfelder KM, Reiser MF, Johnson TRC. Influence of vascular enhancement, age and gender on pulmonary perfused blood volume quantified by dual-energy-CTPA. *Eur J Radiol*. Elsevier Ireland Ltd; 2013; 82: 1565–1570.
22. Kindvall SSI, Diaz S, Svensson J, Wollmer P, Slusarczyk D, Olsson LE. Influence of age and sex on the longitudinal relaxation time, T1, of the lung in healthy never-smokers. *J Magn Reson Imaging*. 2016; 43: 1250–1257. <https://doi.org/10.1002/jmri.25085> PMID: 26558716
23. Jensen RL, Crapo RO. Prediction of normal arterial oxygen levels. *J Investig Med*. 1996; 44. Available: <http://www.scopus.com/inward/record.url?eid=2-s2.0-33749579700&partnerID=tZOtx3y1>
24. Jenkins SC, Moxham J. The effects of mild obesity on lung function. *Respir Med*. 1991; 85: 309–11. Available: <http://www.ncbi.nlm.nih.gov/pubmed/1947368> PMID: 1947368
25. Kershaw LE, Naish JH, McGrath DM, Waterton JC, Parker GJM. Measurement of arterial plasma oxygenation in dynamic oxygen-enhanced MRI. *Magn Reson Med*. 2010; 64: 1838–42. <https://doi.org/10.1002/mrm.22571> PMID: 20677232
26. Hueckel P, Schreiber W, Markstaller K, Bellemann M, Kauczor H-U, Thelen M. Effect of Partial Oxygen Pressure and Hematocrit on T1 Relaxation in Human Blood. *Proceedings of the International Society for Magnetic Resonance in Medicine*. 2000. p. 1586.
27. Silvennoinen MJ, Kettunen MI, Kauppinen R a. Effects of hematocrit and oxygen saturation level on blood spin-lattice relaxation. *Magn Reson Med*. 2003; 49: 568–571. <https://doi.org/10.1002/mrm.10370> PMID: 12594761
28. Zheng S, Xia Y. The impact of the relaxivity definition on the quantitative measurement of glycosaminoglycans in cartilage by the MRI dGEMRIC method. *Magn Reson Med*. 2010; 63: 25–32. <https://doi.org/10.1002/mrm.22169> PMID: 19918900
29. Stanis GJ, Henkelman RM. Gd-DTPA relaxivity depends on macromolecular content. *Magn Reson Med*. 2000; 44: 665–667. PMID: 11064398
30. Li W, Grgac K, Huang A, Yadav N, Qin Q, van Zijl PCMM. Quantitative theory for the longitudinal relaxation time of blood water. *Magn Reson Med*. 2015; 0: n/a–n/a.
31. Blockley NP, Jiang L, Gardener a. G, Ludman CN, Francis ST, Gowland P a. Field strength dependence of R₁ and R2* relaxivities of human whole blood to proance, vasovist, and deoxyhemoglobin. *Magn Reson Med*. 2008; 60: 1313–1320. <https://doi.org/10.1002/mrm.21792> PMID: 19030165
32. Ley S, Puderbach M, Risse F, Ley-Zaporozhan J, Eichinger M, Takenaka D, et al. Impact of oxygen inhalation on the pulmonary circulation: assessment by magnetic resonance (MR)-perfusion and MR-flow measurements. *Invest Radiol*. 2007; 42: 283–290. <https://doi.org/10.1097/01.rli.0000258655.58753.5d> PMID: 17414523
33. Cotes JE, Chinn DJ, Quanjer PH, Roca J, Yernault JC. Standardization of the measurement of transfer factor (diffusing capacity). Report Working Party Standardization of Lung Function Tests, European Community for Steel and Coal. Official Statement of the European Respiratory Society. *Eur Respir J Suppl*. 1993; 16: 41–52. Available: <http://www.ncbi.nlm.nih.gov/pubmed/8499053> PMID: 8499053
34. Jakob PM, Hillenbrand CM, Wang T, Schultz G, Hahn D, Haase A. Rapid Quantitative Lung 1 H T 1 Mapping. *J Magn Reson imaging*. 2001; 14: 795–799. PMID: 11747038
35. Look DC. Time Saving in Measurement of NMR and EPR Relaxation Times. *Rev Sci Instrum*. 1970; 41: 250.
36. Arnold JFT, Fidler F, Wang T, Pracht ED, Schmidt M, Jakob PM. Imaging lung function using rapid dynamic acquisition of T1-maps during oxygen enhancement. *MAGMA*. 2004; 16: 246–53. <https://doi.org/10.1007/s10334-004-0034-z> PMID: 15042464
37. Alamedi FD, Morgan AR, Hubbard Cristinacce PL, Nordenmark LH, Hockings PD, Lagerstrand KM, et al. COPD Patients Have Short Lung Magnetic Resonance T 1 Relaxation Time. *COPD J Chronic Obstr Pulm Dis*. 2015; 2555: 1–7.
38. Hernan MA, Clayton D, Keiding N. The simpson’s paradox unraveled. *Int J Epidemiol*. 2011; 40: 780–785. <https://doi.org/10.1093/ije/dyr041> PMID: 21454324
39. Parsons TJ, Power C, Manor O. Physical activity, television viewing and body mass index: a cross-sectional analysis from childhood to adulthood in the 1958 British cohort. *Int J Obes (Lond)*. 2005; 29: 1212–1221.
40. Nystad W, Samuelsen SO, Nafstad P, Langhammer A. Association between level of physical activity and lung function among Norwegian men and women: The HUNT Study. *Int J Tuberc Lung Dis*. 2006; 10: 1399–1405. PMID: 17167959